

Structure and Stability of Pentafluoroaniline and 4-Aminononafluorobiphenyl Radical Anions: Optically Detected Electron Paramagnetic Resonance, Time-Resolved Fluorescence, Time-Resolved Magnetic Field Effect, and Quantum Chemical Study

Vsevolod I. Borovkov,^{†,‡} Irina V. Beregovaya,^{*,§} Lyudmila N. Shchegoleva,[§] Svetlana V. Blinkova,[†] Dmitry A. Ovchinnikov,^{†,‡} Larisa Yu. Gurskaya,^{||} Vitaly D. Shteingarts,^{§,⊥} Victor A. Bagryansky,^{†,‡} and Yuriy N. Molin[†]

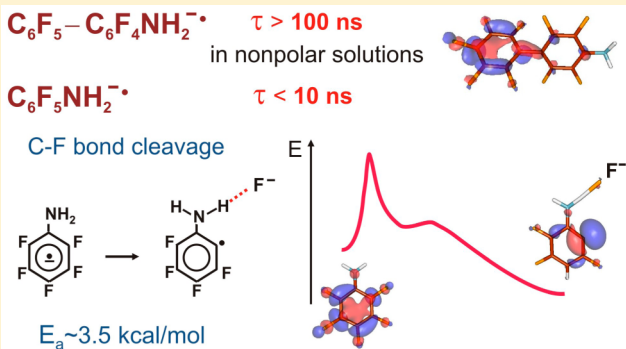
[†]Voevodsky Institute of Chemical Kinetics and Combustion, Siberian Branch of Russian Academy of Science, 3 Institutskaya Street, Novosibirsk 630090, Russia

[‡]Novosibirsk State University, 2 Pirogova Street, Novosibirsk 630090, Russia

[§]N.N. Vorozhtsov Novosibirsk Institute of Organic Chemistry, Siberian Branch of Russian Academy of Science, 9 Lavrentiev Avenue, Novosibirsk 630090, Russia

^{||}Institute of Chemistry Saint Petersburg State University, 26 Universitetskii Prospect, Petrodvorets, Saint-Petersburg 198504, Russia

ABSTRACT: Radical anions (RAs) are the key intermediates of the selective hydrodefluorination of polyfluoroarenes. We used the techniques of optically detected electron paramagnetic resonance (OD EPR), time-resolved fluorescence, time-resolved magnetic field effect (TR MFE), and the density functional theory to study the possibility of RAs formation from 4-aminononafluorobiphenyl (1) and pentafluoroaniline (2) and estimate their lifetimes and decay channels. To our knowledge, both RAs have not been detected earlier. We have registered the OD EPR spectrum for relatively stable in nonpolar solutions $1^{\bullet-}$ but failed to register the spectra for $2^{\bullet-}$. However, we managed to fix the $2^{\bullet-}$ by the TR MFE method and obtained its hyperfine coupling constants. The lifetime of $2^{\bullet-}$ was found to be only a few nanoseconds. The activation energy of its decay was estimated to be 3.6 ± 0.3 kcal/mol. According to the calculation results, the short lifetime of $2^{\bullet-}$ is due to the RA fast fragmentation with the F^- elimination from ortho-position to the amine group. The calculated energy barrier, 3.2 kcal/mol, is close to the experimental value. The fragmentation of $2^{\bullet-}$ in a nonpolar solvent is possible due to the stabilization of the incipient F^- anion by the binding with the amine group proton.



1. INTRODUCTION

Fluorinated arylamines are valuable building blocks in the chemistry of bioactive fluorinated compounds and in particular azaheterocyclic ones. First of all, this concerns readily available mono- and difluoroanilines obtained by traditional techniques for the introduction of fluorine and an amine group in the aromatic ring.^{1–5} Tri- and tetra-fluorinated anilines, however, are much less studied and used because their synthesis by these techniques is multistep and difficult.^{6–8}

The latter is typical of partially polyfluorinated arenes in general. Of late years, the convenient approach to these compounds was developed extensively based on the selective hydrodefluorination of polyfluoroarenes easily available by other methods.^{9–13} Among these techniques, of special attention is the reduction by zinc in aqueous ammonia (the simplest reduction system hitherto used for this purpose), which is believed to occur through the formation of polyfluoroarene radical anions (RAs)^{14,15} followed by their

fragmentation with the elimination of fluoride anion.^{16–18} Thus, the applicability of this system to synthesis is determined by its capability to reduce a polyfluoroarene, while the regioselectivity of the hydrodefluorination is determined by the fragmentation behavior of the respective RA, which justifies the interest to the structure and the properties of polyfluoroarene RAs.

In view of the potential importance of partially fluorinated anilines for synthesis, the possibility of their preparation through this simple technique appears to be quite attractive. Unfortunately, pentafluoroaniline cannot be hydrodefluorinated in the Zn–aqueous ammonia system at room temperature because of insufficient electron affinity. Nevertheless, the hydrodefluorination becomes possible if one uses the more

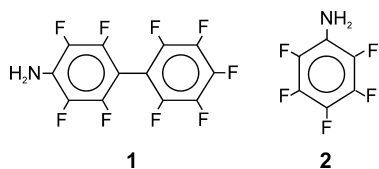
Received: March 18, 2015

Revised: July 8, 2015

Published: July 8, 2015

electrophilic N-acetylpentafluoroanilide due to the suppression of the electron-donating effect of the amine group¹⁶ or a polyfluorinated 2-naphthylamine due to the higher electron affinity of the naphthalene core as compared to the benzene one.¹⁸ However, one cannot rule out that the hydro-defluorination of polyfluoroanilines can be feasible under harsher conditions or as a result of the introduction of substituents raising the benzene ring electron affinity. One can expect that one of such substituents might be the pentafluorophenyl group.

This work is focused on the experimental verification of the possibility of the RA formation from 4-aminononafluorobiphenyl (**1**) and pentafluoroaniline (**2**), the determination of the RAs hyperfine coupling constants and lifetimes as well as the theoretical interpretation of the obtained data using potential energy surface calculations.



RAs of fluorinated benzene derivatives are known to have nontrivial electronic and spatial structure.^{19,20} Fluorine atoms perturb weakly the benzene π -system but strongly perturb the σ -one. The first results are in a small energy splitting of the RA π -states, their terms crossing, and the crossing avoidance through pseudorotation. The second generates the low-lying excited σ -states of the RA that cause the pseudo-Jahn–Teller out-of-plane distortions. The resulting PESes have very complicated multiwell architecture.

The extremely high hyperfine coupling (HFC) constants reflecting the nonplanar structure of the fluoroarene RAs make them the suitable objects for electron paramagnetic resonance (EPR) study. Generally, these RAs are very short-living species so conventional EPR method is not applicable to provide data on their structure. We used the techniques of optically detected EPR (OD EPR), time-resolved fluorescence (TRF), and time-resolved magnetic field effect (TR MFE) for the RAs under study. These methods possessing exceptional sensitivity to radical ions of luminescent molecules enable detection of RAs generated via direct reducing of precursor by excess electrons in irradiated solvent.^{21,22}

2. MATERIALS AND METHODS

2.1. Materials. The following amines were used: 4-aminononafluorobiphenyl (**1**), prepared by the described earlier method,²³ and pentafluoroaniline (**2**), prepared at the experimental chemical plant of the N. N. Vorozhtsov Novosibirsk Institute of Organic Chemistry through the ammonolysis of hexafluorobenzene. As a luminophore for the OD EPR spectra registration, *para*-terphenyl-*d*₁₄ (*p*-TP) was used (99%, Aldrich). Hexamethyldisiloxane (HMDS, 99.5%) and hexafluorobenzene (99%) were received from Aldrich as well. As solvents, dodecane and isooctane were employed after purification by passing through a chromatographic column with aluminum oxide activated with silver nitrate (the purification was performed by N. E. Ivanova, Voevodsky Institute of Chemical Kinetics and Combustion, Siberian Branch of the Russian Academy of Sciences). Before the measurements, oxygen was removed from the solutions through freeze–pump–thaw cycles.

2.2. Methods. The RAs under study were generated by continuous or pulsed X-ray irradiation of alkane solutions of precursors. Solvent ionization produces geminate spin-correlated electron/solvent radical cation pairs. Polyfluoroarene molecules capture the excess electrons. The RAs thus derived further recombine with the radical cation (RC) or another positive charge carrier that could be formed to the moment. Upon the recombination of singlet-state radical ion pairs (RIPs), delayed fluorescence is generated.

2.2.1. Optically-Detected EPR. The OD EPR spectrum was registered by measuring the fluorescence intensity of the recombination products of the RIPs changing with the external magnetic field under continuous X-ray and microwave irradiations. The close connection to conventional EPR technique originates from the resonant MW-induced transitions between spin states of spin-correlated geminate RIPs. The resonant conditions relate to HFCs of the radicals in the same way as in EPR technique.

The measurements were carried out on a device based on a Bruker ER-200D EPR spectrometer equipped with an ionizing radiation source (an X-ray tube), a photomultiplier to measure fluorescence intensity, and a microwave amplifier.²⁴ The microwave power was set to 2.5 W and a modulation magnitude of the external magnetic field was of 0.36 mT. To determine the hyperfine coupling constants, the measured optically detected EPR spectra were simulated using WinSim-2002 program.²⁵

2.2.2. Time-Resolved Recombination Fluorescence and Time-Resolved Magnetic Field Effect. The time-resolved fluorescence from the studied alkane solutions was registered by the single-photon counting technique using a nanosecond X-ray fluorimeter²⁶ with exciting X-ray pulses of about 1 ns long with a typical energy of quanta of about 20 keV. The temperature of the samples was stabilized within ± 1 °C.

The TR MFE is the ratio between the kinetics of recombination fluorescence measured with and without magnetic field. The evolution of spin state of geminate RIPs depends on both HFCs of radical ions and magnetic field thus providing, in essence, the same information on the radicals as OD EPR. The great advantage of the TR MFE method is the potential ability to observe radical ions with extremely short (about a few nanoseconds) lifetime.

The time-resolved experiments were performed in isooctane as a solvent. In TR MFE experiments, the HMDS addition provides fast capture of the solvent RCs and reduces the effect of HFCs in isooctane RC on the TR MFE curve clarifying thus the relative contribution of HFCs in RAs. Typical EPR spectra width ($\sigma^2 = 1/3(\sum_i a_i^2 I(I+1))$) for the isooctane RC, $\sigma = 2.1$ mT,²⁷ whereas for the HMDS RC it is no more than ~ 0.3 mT by our estimations. Therefore, HFCs of the HMDS RC appear on the times larger than 20–30 ns. Besides, HMDS virtually does not affect the electron moving and recombination kinetics of RIPs in irradiated solutions.

2.2.3. Quantum Chemical Calculations. The potential energy surface (PES) calculations were made in the adiabatic approximation using the density functional theory with the B3LYP and CamB3LYP functionals in the spin-restricted variant and standard 6-31+G* basis set. Stationary points of the PES were located, and their type was determined from the analysis of normal vibrations. The interrelations between the stationary points were established using intrinsic reaction coordinate (IRC) calculations. Solvent effect was accounted for

by the CPCM technique using cyclohexane and H₂O as model solvents.

The calculations of the ¹⁹F HFC constants for stationary RA structures were performed using the same functionals in the spin-unrestricted variant. Taking into consideration the previous experience,^{28,29} we used the gas-phase calculation results.

All the calculations were made with the GAMESS package.³⁰

2.2.4. Hydrodefluorination of the Amine 1 by Zinc in Aqueous Ammonia. To a solution of CuCl₂ (0.406 g, 3.02 mmol) in 30% aqueous ammonia (25 mL) cooled down to 0 °C, zinc powder (0.590 g, 9.06 mmol) was added and the mixture was stirred for 10 min. Then 4-aminononafluorodiphenyl (0.200 g, 0.60 mmol) was added and the mixture was further stirred for 24 h at room temperature. The precipitate was filtered off, washed with water (2 × 10 mL) and dichloromethane (4 × 10 mL), the combined liquor was extracted with dichloromethane (2 × 10 mL). The extract was dried with MgSO₄ and the solvent was evaporated. According to the ¹⁹F NMR (acetone, C₆F₆ internal) and GC/MS analyses, the solid residue (0.18 g) contained 95% of the starting compound and 5% of previously reported 4-amino-2,3,5,6,2',3',5',6'-octafluorobiphenyl.¹⁶

3. RESULTS AND DISCUSSION

3.1. Time-Resolved Fluorescence Experiments. Figure 1 shows the delayed fluorescence decay curves as generated by

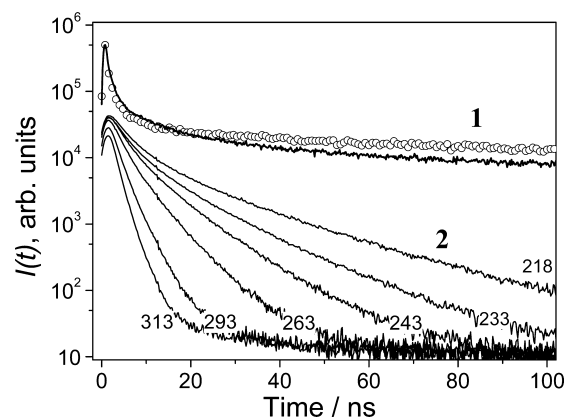


Figure 1. Recombination fluorescence intensity decay curves, $I(t)$, from irradiated 2 mM solutions of **1** (upper curves) and **2** (lower curves) in isoctane at different temperatures. For **2**, the temperature values are shown at the particular curves. The curves are normalized approximately to the equal irradiation dose. For **1**, the temperatures are 233 (solid line) and 323 K (circles).

X-ray irradiation of isoctane solutions of the amines studied at room temperature. Very high electron mobility in isoctane ensures extremely fast formation of the fluoroarene RAs. Unscavenged electrons should recombine too fast to be detected on the time scale longer than 1 ns. Note that photophysical properties of the solutes are not investigated in detail yet, however, only relatively short-lived luminescent states are of importance for this work. In this case, the fluorescence intensity decay, $I(t)$, almost exactly reproduces the time dependence of the recombination rate of geminate RIPs.

The data shown in Figure 1 clearly demonstrate a qualitative difference between the fluoroarenes studied. The curves obtained for **1** exhibit nearly hyperbolic time dependence

typical for the recombination of geminate RIPs within the whole temperature range studied. The dependence of the $I(t)$ curves on temperature mostly relates to the RA mobility dependence on the solution viscosity.

On the contrary, $I(t)$ curves obtained for **2** becomes nearly exponential already in a few nanoseconds after irradiation. This testifies that one of the partners of the geminate RIP is involved to some parallel monomolecular process. Keeping in mind that the experiment conditions are the same for **1** and **2**, we can conclude that this partner is $2^{\bullet-}$. The RA monomolecular transformation may be a reason for its much shorter lifetime in comparison with $1^{\bullet-}$.

3.2. Structure of the Radical Anions. 4-Aminononafluorobiphenyl Radical Anion. Figure 2 shows the OD EPR

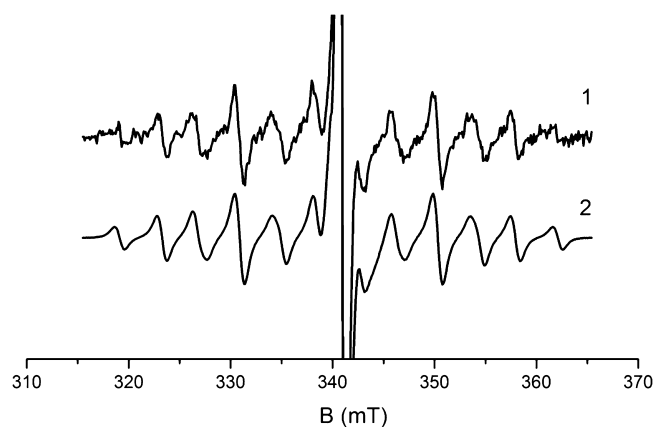


Figure 2. (1) OD EPR spectrum of the solution of 7×10^{-4} M of **1** with 1×10^{-3} M *p*-TP in dodecane at room temperature. (2) Simulation of the OD EPR spectrum with the HFC parameters $a_1(2F) = 4.2$ mT, $a_2(2F) = 7.6$ mT, $a_3(F) = 19.4$ mT, $\Delta H_{pp} = 0.93$ mT for $1^{\bullet-}$ and $\Delta H_{pp} = 0.35$ mT for *p*-TP^{•+} radical ions (Gaussian line shape).

spectrum of the solution of 7×10^{-4} M of **1** in dodecane containing 10^{-3} M *p*-TP as a fluorophore to enhance the solution luminosity. The spectrum consists of a narrow central line and a multiplet with rather large HFC constants. The central line belongs to the *p*-TP radical ions. The multiplet can be attributed to $1^{\bullet-}$ and described well by the hyperfine interaction at the three groups of fluorine nucleus with HFC constants $a_1(2F) = 4.2$ mT, $a_2(2F) = 7.6$ mT, $a_3(F) = 19.4$ mT. The HFC constants with the ¹H and ¹⁴N nuclei in $1^{\bullet-}$ are small and contribute to the widths of the lines.

The results of TR MFE measurements are presented in Figure 3 that shows the data obtained for solution of 10^{-3} M of **1** in isoctane with HMDS added in relatively large concentration, 0.1 M. Solid line in Figure 3 shows the results of the best fit simulation of the TR MFE curve for the pairs ($1^{\bullet-}$ /RC) with $\sigma_c \sim 0.1$ mT for the RC. The ¹⁹F HFC constant values and times of phase paramagnetic relaxation for radical ions were varied independently. Note that the values of the paramagnetic relaxation times, which turned out to be rather short, affect only the oscillation amplitudes but not their positions.³¹ The latter are determined by HFC in RA. Good agreement between the HFC constant values resulting from simulation of the TR MFE curve and the OD EPR spectra (see captions to Figures 2 and 3) testifies that the same particle is observed in both experiments.

For interpreting the above experimental data, quantum chemical calculations have been carried out. We have built the

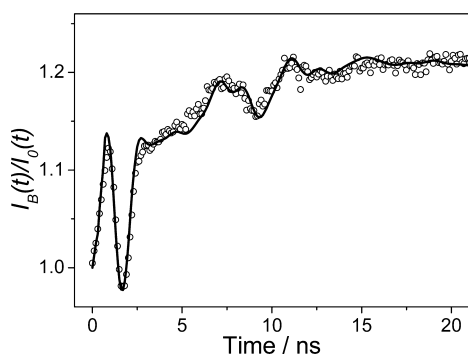


Figure 3. Curve of TR MFE for solutions of 2 mM of **1** in isoctane with addition of 0.1 M of HMDS (circles) measured at room temperature and its simulations (solid line) in a model with $a_1(2F) = 4.1$ mT, $a_2(2F) = 7.2$ mT, $a_3(F) = 19$ mT for RA and $\sigma = 0.1$ mT for unresolved EPR spectra of RC. Magnetic field strength was of 0.3 T. In the simulation, the fluorescence time of 0.1 ns and the instrument response function with fwhm = 1 ns was taken in account. The phase paramagnetic relaxation time was equal to 4.5 ns.

full PES scheme for $1^{\bullet-}$ following the previous study on the decafluorobiphenyl RA PES.²⁸ The presence of the electron-donating para-amino group results in nearly complete localization of the unpaired electron in the pentafluorophenyl moiety. According to the obtained data, the lowest-energy conformational transition of $1^{\bullet-}$ is due to the phenyl rings mutual rotation. The respective transition state reveals a structure with nearly perpendicular ring planes with the height of the energy barrier being 2.6 kcal/mol.

Figure 4 shows the structure corresponding to one of the four PES minima of $1^{\bullet-}$ (when neglecting the amine group

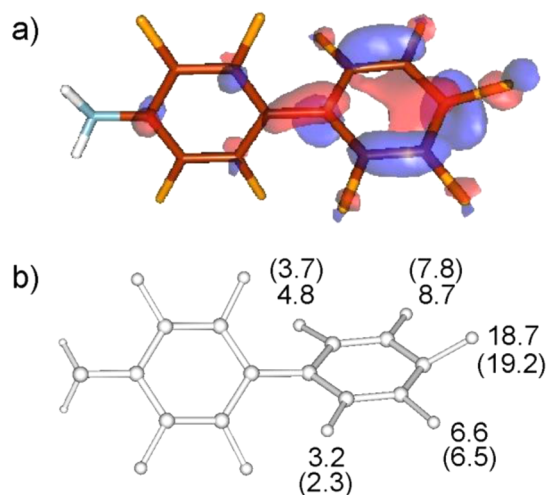


Figure 4. Calculation results for $1^{\bullet-}$: SOMO view (a) and the HFC constants a_F values (b). The a_F values calculated for the gas phase by the UB3LYP and UCamB3LYP (in parentheses) methods are given in mT.

inversion the minima are equivalent). The angle between the ring planes is of 48° , and the fluorine atoms out-of-plane deviations reflect the distribution of the unpaired electron density localized mainly at the position 4'. The distortion of the RA planar structure leads to extremely high HFC constants with the ^{19}F nuclei.³² The calculated constants are shown in Figure 4.

Note that the energy barriers between the structures are low enough to provide the almost complete averaging the HFC constants at temperatures within the studied range. Averaging the calculated a_F values (see Figure 3) by the rings rotation under assumption of fast spectral exchange gives the values $\bar{a}_1(F2', F6') = 4.0$ (3.0) mT, $\bar{a}_2(F3', F5') = 7.7$ (7.2) mT, $\bar{a}_3(F4') = 18.7$ (19.2) mT, which are in a good agreement with the experiment. Thus, the results of quantum chemical calculations allow us to identify undoubtedly the species observed in OD EPR and TR MFE experiments as $1^{\bullet-}$.

Pentafluoroaniline Radical Anion. Attempts to register the EPR spectrum for RA of **2** using OD EPR in a number of nonpolar solvents (squalane, dodecane, isoctane) in the temperature range of 240–310 K were unsuccessful. Results of the TRF experiments (see 3.1) suggest that the OD EPR spectrum could not be detected because of the short lifetime of $2^{\bullet-}$. However, the lifetime is not so short to prevent magnetic field effects revealing in the TR MFE experiments.

Figure 5 shows an example of the TR MFE curve for 2 mM solutions of amine **2** in isoctane with added HMDS at 273 K.

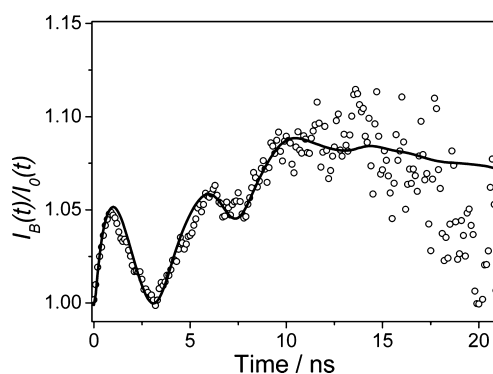


Figure 5. Curve of TR MFE for solutions of 2 mM of **2** (circles) in isoctane (+0.1 M HMDS added) measured at 273 K and its simulation (solid line) in a model of unresolved EPR spectra of radical cation ($\sigma = 0.1$ mT) and HFC constants in RA equaled to $a_1(2F) = 10.5$ mT, $a_2(2F) = 16$ mT, $a_3(F) = 14.5$ mT. Magnetic field strength was of 0.3 T. In the simulation, fluorescence time of 0.5 ns and instrument function with fwhm = 1 ns was taken in account. The phase relaxation time was equal to 4 ns.

Because of the high rate of fluorescence intensity decay of the **2** solutions, a distinct signal can be observed only up to 10 ns. Nevertheless, the rate of the singlet–triplet transitions is high enough to provide the appearance of some oscillations at the TR MFE curves. This indicates the presence of large HFC constants for one of the geminate RIP partner. This suggests that this partner may be $2^{\bullet-}$. So, we used the HFC constants calculated for this RA (see below) as starting values for simulation of the TR MFE curves. The best fit constant values are given in the capture in Figure 5.

Earlier we have shown that $2^{\bullet-}$ is structurally flexible.¹⁶ Its PES has the form of a pseudorotation surface with a trough comprising 12 nonplanar stationary structures: six minima and six transition states (Figure 6a). The scheme of the PES is similar to that for the hexafluorobenzene RA³³ with the structure notations being assigned earlier.¹⁹ The energy minima correspond to structures $B(\pm\pi/3)^+$ and $B(\pm\pi/3)^-$ (with an energy difference of 0.2 kcal/mol) dissimilar in the amine group inversion (Table 1, Figure 6a). The SOMOs of these structures are localized at the ring positions 3 and 6 or 2 and 5. The

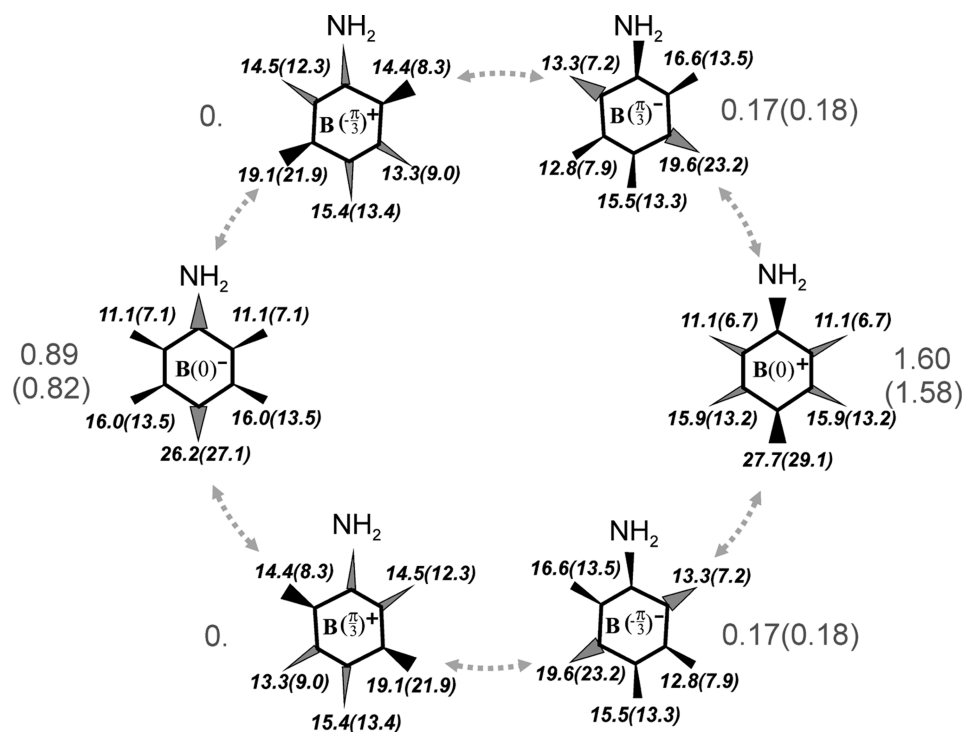


Figure 7. Relative energies and HFC constants for the $2^{-\bullet}$ PES minima calculated for a gas phase by the UB3LYP and UCamb3LYP (in parentheses) methods. ΔE values are given in kcal/mol and a_F in mT.

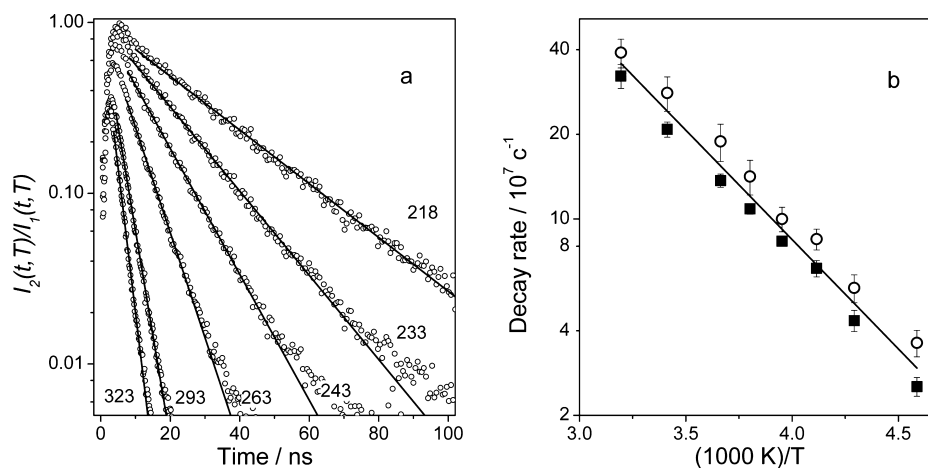


Figure 8. (a) Ratios of experimental fluorescence decay curves (circles) obtained for solutions of **2**, $I_2(t)$, and those for solutions of **1**, $I_1(t)$, at the temperatures indicated in the plot. Solid lines show exponential approximation of the curves. (b) A plot of the $2^{-\bullet}$ decay rate dependence on $1000/T$ in semilogarithmic scale obtained with the fluorescence decay ratios given in the panel a (circles) and with the analogous ratios measured for the isooctane solutions of hexafluorobenzene instead of **1** (squares).

$A(0)^\pm$, $A(\pm\pi/3)^\pm$, the height of the barriers along the pseudorotation path being in the range 0.3–1.4 kcal/mol.

Such surface flatness definitely demands HFC constant to be averaged over the whole pseudorotation path. But as the first step, here we have averaged the constant values over the PES minima only (Figure 7) within the classical Boltzmann distribution. The resulting \bar{a}_i values depend strongly on the functional used. B3LYP yields the values $\bar{a}_{\text{ortho.}}(2F) = 10.2 \text{ mT}$, $\bar{a}_{\text{meta.}}(2F) = 17.1 \text{ mT}$, $\bar{a}_{\text{para.}}(F) = 21.7 \text{ mT}$, the latter being too high in comparison with the experimental one. Meanwhile, the CamB3LYP results ($\bar{a}_{\text{ortho.}}(2F) = 10.1 \text{ mT}$, $\bar{a}_{\text{meta.}}(2F) = 15.4 \text{ mT}$, $\bar{a}_{\text{para.}}(F) = 14.4 \text{ mT}$) agree closely with the experimental ones (see the caption to Figure 5 for the experimental $a(F)$

values). This result strongly supports the assignment of the TR MFE curves to $2^{-\bullet}$.

3.3. Stability of Radical Anions. Pentafluoroaniline Radical Anion. As shown above by the TRF experiments, the RA $2^{-\bullet}$ reveals much shorter lifetime in comparison with $1^{-\bullet}$, which is stable under the experimental conditions. Assuming that polyfluoroarene RAs possess the close rates of disappearing via the geminate recombination we can estimate the rate of $2^{-\bullet}$ decay via the parallel chemical process using a fluorescence decay curve for some acceptor giving a stable RA.³⁴ Such approach is approximate, so the use of several reference RAs increases accuracy of estimate. We use as a reference the fluorescence decay curves, $I_1(t)$, obtained for alkane solutions of **1** and hexafluorobenzene.

The ratios of the fluorescence decay curves, $I_2(t)/I_1(t)$, obtained for solutions of **2** and **1** are shown in Figure 8a for various temperatures. Starting from a few nanoseconds, these ratios may be approximated well by an exponent thus indicating the monomolecular character of the $2^{\bullet-}$ decay. This allows us to obtain the temperature dependence of the decay rate shown by circles in Figure 8b. Analogous dependence obtained from the data for the hexafluorobenzene solution instead of **1** is depicted by squares. The activation energy of $2^{\bullet-}$ decay was determined from the straight line slopes in Figure 8b as 3.6 ± 0.3 kcal/mol being only slightly dependent on the reference choice. The mean value of the pre-exponent was found to be $1.1 \times 10^{11} \text{ s}^{-1}$. So the lifetime of $2^{\bullet-}$ is about several nanoseconds, which is below the detection limit for the OD EPR method. This is the reason for the technique failure in $2^{\bullet-}$ registering.

The TRF technique provides no information on the decay channel of $2^{\bullet-}$. As known, the main way of the polyfluoroarene RA cleavage in polar media is fragmentation with the fluoride ion elimination.³⁵ We performed quantum chemical calculations in order to estimate whether this kind of decay is possible in a nonpolar solvent.

It was shown previously that **2** cannot be defluorinated by zinc in aqueous ammonia that was attributed to its insufficient electron affinity.¹⁶ We theoretically discussed the fragmentation of RA $2^{\bullet-}$ at the para-position to the amine group believing it to be the most probable for a polar medium.¹⁶ However, the present CPCM calculations with cyclohexane as a model solvent demonstrate that in nonpolar media the fragmentation of this RA should occur at the ortho-position. This seems quite natural as the incipient fluoride anion is stabilized due to intramolecular binding with the amine group proton eventually forming an HF molecule. Such binding plays the key role for the gas-phase dissociative electron attachment to pentafluoroaniline as well.^{36,37} The HF loss was also observed as the most intense signal from pentafluoroaniline in low energy electron capture reactions in gas phase under negative chemical ionization conditions.³⁸

We found local PES minima lying outside the pseudorotation trough and corresponding to structures where one of the C–F ortho-bonds is markedly elongated ($R_{\text{CF}} = 2.29 \text{ \AA}$) due to its interaction with the NH_2 group. The corresponding SOMOs are an antibonding σ -orbital of the elongated bond, therefore we will use the notation S_{CF} for these structures (Table 1 and Figure 6a). The energy of the local minima found is only 0.7 kcal/mol higher than the energy of the minima $\text{B}(\pm\pi/3)^{\pm}$. The minima S_{CF} and $\text{B}(\pm\pi/3)^{\pm}$ are separated by transition states TS_I (Figure 6, Table 1). The corresponding energy barrier is 3.0 kcal/mol, which is almost the same as the activation energy of the RA $2^{\bullet-}$ decay obtained experimentally.

Further moving along the reaction coordinate leads to growing charge localization at the fluorine atom leaving and does not require any considerable energy. At $R_{\text{CF}} = 2.50 \text{ \AA}$, the second transition state (TS_II) is located having a relative energy 0.9 kcal/mol. The formation of a bond between the incipient fluoride ion and the hydrogen of the amine group lowers the total energy of the system relative to the S_{CF} minima by 2.2 kcal/mol. As a result, the global PES minima of $2^{\bullet-}$ are hydrogen-bonded complexes formed by the fluoride ion and 2-amino-3,4,5,6-tetrafluorophenyl radical (Table 1, Figure 6).

The decay of $2^{\bullet-}$ with the fluoride ion elimination from the para-position to NH_2 group is most probable for structures $\text{B}(0)^{\pm}$. Reaction coordinate calculations performed for the

lower energy structure $\text{B}(0)^{-}$ showed that in a nonpolar solvent, as well as in gas phase,¹⁶ the elongation of the para-C–F bond leads to a monotonous energy growth. As R_{CF} changing from 1.47 to 2.8 \AA , the total energy of the system grows by ~ 12 kcal/mol; therefore this decay channel is unfavorable energetically. Exactly the same situation occurs for the fluoride ion elimination from the meta-position when starting from the $\text{B}(\pi/3)^+$ structure. Thus, the possibility of the fragmentation of $2^{\bullet-}$ in a low polar medium is solely due to the stabilization of the incipient fluoride anion through its binding with the amine group proton.

4-Aminononafluorobiphenyl Radical Anion. Under conditions of the TRF experiments with nonpolar alkane solvents RA $1^{\bullet-}$ is stable. Obviously, the prevailing location of the unpaired electron in the pentafluorophenyl ring (Figure 4) excludes the fragmentation of this RA at the ortho-position to the NH_2 group predicted by calculations for $2^{\bullet-}$. Besides, the special experiments (see Section 2.2.4) showed that in accordance with the structure of $1^{\bullet-}$ represented in Figure 4, the product of the amine **1** hydrodefluorination by zinc in aqueous ammonia is 4-amino-4'-H-octafluorobiphenyl. Thus, the RA defluorination channel in a polar solvent is determined by the distribution of the unpaired electron density and the type of the out-of-plane distortion.

According to our CPCM calculations with water as a model solvent, the PES section of $1^{\bullet-}$ along the coordinate of the C_4 –F bond stretching is rather flat. On the potential energy curve, there is an extremely shallow minimum with an elongated C_4 –F bond ($R_{\text{C}_4\text{F}} = 1.94 \text{ \AA}$) related to a structure with the charge partially transferred to the fluorine atom ($q_{\text{F}} \sim -0.6$). Its energy is only 0.6 kcal/mol higher than that of the global minimum, the barrier between the two minima being of 0.7 kcal/mol. However, further elongation of the bond raises the total energy of the system (the calculations were performed using the reaction coordinate technique up to $R_{\text{C}_4\text{F}} = 3.5 \text{ \AA}$, $q_{\text{F}} \sim -1$, $\Delta E \sim 5$ kcal/mol). This energy disadvantage of F^- elimination from the 4'-position of $1^{\bullet-}$ is apparently due to the specific solvation ignoring.

4. CONCLUSIONS

The possibility of the formation of $1^{\bullet-}$ and $2^{\bullet-}$ and their decay channels were studied by the techniques of optically detected EPR, time-resolved recombination fluorescence, time-resolved magnetic field effect, and the density functional theory.

The EPR spectrum of $1^{\bullet-}$ was registered for the first time in liquid alkanes by the OD EPR method. The HFC constant values resulting from simulation the OD EPR spectra and TR MFE curve are in a good agreement. According to the TRF data this RA is stable in nonpolar solutions for hundreds of nanoseconds.

We failed to register the OD EPR spectra of $2^{\bullet-}$. However, we have managed to fix $2^{\bullet-}$ by the TR MFE method and to estimate the HFC constants values. The lifetime of this RA in the alkane solutions was found to be only a few nanoseconds. The temperature dependence of the decay rate constant for $2^{\bullet-}$ was measured and the respective activation energy was estimated to be 3.6 ± 0.3 kcal/mol. To our knowledge, this RA has not been detected earlier.

The quantum chemical calculation performed showed that the RAs studied have complex multiwell PESes. The complicated PES structure must be accounted for at the HFC parameters interpretation and at analyzing the RA defluorination selectivity. Interpreting the HFC parameters obtained from

the simulation of 1^{\bullet} OD EPR spectrum requires accounting for the flexibility of this RA structure with respect to a mutual rotation of the benzene rings. The HFC constant averaging over the PES minima for 2^{\bullet} resulted in values close to the experimental ones. By the data of calculations, the short lifetime of 2^{\bullet} is due to the RA fast fragmentation with the elimination of the fluoride ion from the ortho-position to the amine group, and the estimated energy barrier of 3.0–3.4 kcal/mol is close to the experimental value. The fragmentation of 2^{\bullet} in a nonpolar solvent is possible due to the stabilization of the incipient F^- anion by the binding with the amine group proton.

AUTHOR INFORMATION

Corresponding Author

*E-mail: ivb@nioch.nsc.ru. Tel: +7(383)330-78-64. Fax: +7-383-330-9752.

Notes

The authors declare no competing financial interest.

[†](V.D.S.) Deceased February 12, 2015.

ACKNOWLEDGMENTS

The work was supported by Russian Foundation for Basic Researches (RFBR) under Grant 13-03-000427 and by the Program “Leading Scientific Schools” (project NS-5744.2014.3). Synthetic work was supported by RFBR, Grant 14-03-00108. Authors are thankful to K. S. Taletsky for help in numeric simulation of MFE curves.

REFERENCES

- (1) *Organofluorine Compounds in Medical Chemistry and Biomedical Applications*; Filler, R., Kobayashi, Y., Yagupolskii, L. M., Eds.; Elsevier: Amsterdam, 1993.
- (2) *Organofluorine Chemistry. Principles and Commercial Applications*; Banks, R. E.; Smart, B. E., Tatlow, J. C., Eds.; Plenum Press: New York, 1994.
- (3) Kirk, K. L. Fluorine in Medicinal Chemistry: Recent Therapeutic Applications of Fluorinated Small Molecules. *J. Fluorine Chem.* **2006**, *127*, 1013–1029.
- (4) Isanbor, C.; O'Hagan, D. Fluorine in Medicinal Chemistry: a Review of Anticancer Agents. *J. Fluorine Chem.* **2006**, *127*, 303–319.
- (5) *Fluorine in Medicinal Chemistry and Chemical Biology*; Ojima, I., Ed.; Wiley-Blackwell: Chippinham, 2009.
- (6) Florin, R. E.; Pummer, W. J.; Wall, L. A. Reaction of Aromatic Fluoro-Carbons with Hydrogen. *J. Res. Natl. Bur. Standards* **1959**, *62*, 107–112.
- (7) Belf, L. G.; Buxton, M. W.; Tilney-Bassett, J. F. Some Reactions of 1,2,3,4-Tetrafluorobenzene and Derived Compounds. *Tetrahedron* **1967**, *23*, 4719–4727.
- (8) Petrova, T. D.; Mamaev, V. P.; Yakobson, G. G. Polyfluoroaromatic Compounds in the Fischer Reaction. *Izv. Akad. Nauk SSSR, Ser. Khim.* **1969**, *3*, 679–682.
- (9) Kiplinger, J. L.; Richmond, T. G.; Osterberg, C. E. Activation of Carbon-Fluorine Bonds by Metal Complexes. *Chem. Rev.* **1994**, *94*, 373–431.
- (10) Alonso, F.; Beletskaya, I. P.; Yus, M. Metal-Mediated Reductive Hydrodehalogenation of Organic Halides. *Chem. Rev.* **2002**, *102*, 4009–4091.
- (11) Shteingarts, V. D. Recent Advances in Practice and Theory of Polyfluoroarene Hydrodehalogenation. *J. Fluorine Chem.* **2007**, *128*, 797–805.
- (12) Amii, H.; Uneyama, K. C–F Bond Activation in Organic Synthesis. *Chem. Rev.* **2009**, *109*, 2119–2183.
- (13) Kuehnle, M. F.; Lentz, D.; Braun, T. Synthesis of Fluorinated Building Blocks by Transition-Metal-Mediated Hydrodefluorination Reactions. *Angew. Chem., Int. Ed.* **2013**, *52*, 3328–3348.
- (14) Handoo, K. L.; Gadru, K. Zn/OH Reductions of Organic Compounds in Dimethylsulfoxide; A New Simple Method of Preparing Radical Anions. *Tetrahedron Lett.* **1986**, *27*, 1371–1372.
- (15) Gerson, F.; Gescheidt, G.; Haring, P.; Mazur, Y.; Freeman, D.; Spreitzer, H.; Daub, J. Electron-Acceptor Properties of Hypericin and Its Salts: An ESR/ENDOR and Electrochemical Study. *J. Am. Chem. Soc.* **1995**, *117*, 11861–11866.
- (16) Laev, S. S.; Gurskaya, L. Yu.; Selivanova, G. A.; Beregovaya, I. V.; Shchegoleva, L. N.; Vasil'eva, N. V.; Shakirov, M. M.; Shteingarts, V. D. N-Acetylation as a Means to Activate Polyfluoroarylamines for Selective ortho-Hydrodefluorination by Zinc in Aqueous Ammonia: A Concise Route to Polyfluorobenzo Azaheterocycles. *Eur. J. Org. Chem.* **2007**, *2*, 306–316.
- (17) Reshetov, A. V.; Selivanova, G. A.; Politanskaya, L. V.; Beregovaya, I. V.; Shchegoleva, L. N.; Vasil'eva, N. V.; Bagryanskaya, I. Yu.; Shteingarts, V. D. Hydrodefluorination of N-Acetylheptafluoro-2-naphthylaminebyzinc in Aqueous Ammonia: Synthetic Outcomes and Mechanistic Considerations. *J. Fluorine Chem.* **2011**, *8*, 242–262.
- (18) Selivanova, G. A.; Reshetov, A. V.; Beregovaya, I. V.; Vasil'eva, N. V.; Bagryanskaya, I. Yu.; Shteingarts, V. D. Hydrodefluorination of Polyfluoro-2-naphthylamines by Zn in Aqueous NH₃: a Correlation of the Product Distribution and the Computationally Predicted Regioselectivity of the Substrate Radical Anion Fragmentation. *J. Fluorine Chem.* **2012**, *137*, 64–72.
- (19) Beregovaya, I. V.; Shchegoleva, L. N. Potential Energy Surfaces of Fluorobenzene Radical Anions. *Int. J. Quantum Chem.* **2002**, *88*, 481–488.
- (20) Barlukova, M. M.; Beregovaya, I. V.; Vysotsky, V. P.; Shchegoleva, L. N.; Bagryansky, V. A.; Molin, Yu. N. Intramolecular Dynamics of 1,2,3-Trifluorobenzene Radical Anions as Studied by OD ESR and Quantum-Chemical Methods. *J. Phys. Chem. A* **2005**, *109*, 4404–4409.
- (21) Borovkov, V.; Stass, D.; Bagryansky, V.; Molin, Y. Study of Spin-Correlated Radical Ion Pairs in Irradiated Solutions by Optically Detected EPR and Related Techniques. In *Applications of EPR in Radiation Research*; Lund, A., Shiotani, M., Eds.; Springer International Publishing: New York, 2014; pp 629–663.
- (22) Molin, Yu. N.; Anisimov, O. A.; Melekhov, V. I.; Smirnov, S. N. Optically Detected Electron Spin Resonance Studies of Electrons and Holes Involved into Geminate Recombination in Non-Polar Solutions. *Faraday Discuss. Chem. Soc.* **1984**, *78*, 289–301.
- (23) Vaganova, T. A.; Kusov, S. Z.; Rodionov, V. I.; Shundrina, I. K.; Malykhin, E. V. Selective Mono- and Diamination of Polyfluorinated Benzenes and Pyridines with Liquid Ammonia. *Russ. Chem. Bull.* **2007**, *56*, 2239–2246.
- (24) Molin, Yu. N.; Anisimov, O. A. Optical Detection of EPR Spectra from Short-Lived Radical-Ion Pairs in Spurs under Radiolysis. *Radiat. Phys. Chem.* **1983**, *21*, 77–82.
- (25) Duling, D. R. Simulation of Multiple Isotropic Spin-Trap EPR Spectra. *J. Magn. Reson., Ser. B* **1994**, *104*, 105–110.
- (26) Anishchik, S. V.; Grigoryants, V. M.; Shebolaev, I. V.; Chernousov, Y. D.; Anisimov, O. A.; Molin, Yu. N. Pulsed X-ray Fluorimeter with Nanosecond Resolution. *Prib. Tekh. Eksp.* **1989**, *4*, 74–79.
- (27) Borovkov, V. I.; Potashov, P. A.; Shchegoleva, L. N.; Bagryansky, V. A.; Molin, Yu. N. Radical Cations of Branched Alkanes as Observed in Irradiated Solutions by the Method of Time-resolved Magnetic Field Effect. *J. Phys. Chem. A* **2007**, *111*, 5839–5844.
- (28) Shchegoleva, L. N.; Beregovaya, I. V. Manifestation of Complicated Structure of Potential Energy Surfaces in Spectral and Chemical Properties of Haloarene Radical Ions. *Fluorine Notes* **2013**, *2* (87).
- (29) Beregovaya, I. V.; Shchegoleva, L. N. Pseudorotation as a Mechanism for Intramolecular Electron Density Transfer. Fragmentation of the Octafluoronaphthalene Radical Anion. *J. Fluorine Chem.* **2014**, *163*, 1–6.
- (30) Schmidt, M. W.; Baldrige, K. K.; Boatz, J. A.; Elbert, S. T.; Gordon, M. S.; Jensen, J. H.; Koseki, S.; Matsunaga, N.; Nguyen, K. A.

Su, S. J.; et al. General Atomic and Molecular Electronic Structure System. *J. Comput. Chem.* **1993**, *14*, 1347–1363.

(31) Bagryansky, V. A.; Borovkov, V. I.; Molin, Y. N. Quantum Beats in Radical Pairs. *Russ. Chem. Rev.* **2007**, *76*, 493–506.

(32) Schastnev, P. V.; Shchegoleva, L. N. *Molecular Distortions in Ionic and Excited States*. CRC Press: Boca Raton, New York, London, Tokyo, 1995.

(33) Shchegoleva, L. N.; Beregovaya, I. V.; Schastnev, P. V. Potential Energy Surface of $C_6F_6^-$ Radical Anion. *Chem. Phys. Lett.* **1999**, *312*, 325–332.

(34) Bally, T.; Miller, B.; Gerson, F.; Qin, X.-Z.; von Seebach, M.; Kozhushkov, S. I.; de Meijere, A.; Borovkov, V. I.; Potashov, P. A. Radical Cations from Dicyclopropilidenemethane and its Octamethyl Derivative. *J. Phys. Chem. A* **2006**, *110*, 1163–1170.

(35) Shteingarts, V. D.; Kobrina, L. S.; Bilkis, I. I.; Starichenko, V. F.; *Chemistry of Polyfluoroarenes: Reaction Mechanisms and Intermediates*; Nauka: Novosibirsk, 1991 (in Russian).

(36) Ómarsson, B.; Bjarnason, E. H.; Ingólfsson, O.; Haughey, S.; Field, T. A. Chemical Control through Dissociative Electron Attachment – A Study on Pentafluorotoluene, Pentafluoroaniline and Pentafluorophenol. *Chem. Phys. Lett.* **2012**, *539–540*, 7–10.

(37) Ómarsson, B.; Bjarnason, E. H.; Haughey, S.; Field, T. A.; Abramov, A.; Klüpfel, P.; Jónsson, H.; Ingólfsson, O. Molecular Rearrangement Reactions in the Gas Phase Triggered by Electron Attachment. *Phys. Chem. Chem. Phys.* **2013**, *15*, 4754–4766.

(38) Gregor, I.; Guilhaus, M. Gas Phase Electron Attachment Reactions and Negative Ion Mass Spectra of Substituted Pentafluorophenyl Compounds. *J. Fluorine Chem.* **1983**, *23*, 549–556.